Carbohydrate Polymers 106 (2014) 132–141

Contents lists available at ScienceDirect

Carbohydrate Polymers

journal homepage: www.elsevier.com/locate/carbpol

Physical, structural, mechanical and thermal characterization of bacterial cellulose by *G. hansenii* NCIM 2529

Bhavna V. Mohite, Satish V. Patil*

School of Life Sciences, North Maharashtra University, P.O. Box 80, Jalgaon 425001, MS, India

ARTICLE INFO

Article history:
Received 28 September 2013
Received in revised form 4 February 2014
Accepted 5 February 2014
Available online 14 February 2014

Keywords:
Biopolymer
Agitation
Thermogravimetric
Water holding capacity
DSC

ABSTRACT

The present study aims to investigate the physico mechanical, structural and thermal properties of the bacterial cellulose (BC) produced under shaking condition. Formation of characteristic cellulose sphere has been characterized by light and scanning electron microscopy. The purity of bacterial cellulose was confirmed by thin layer chromatography of hydrolyzed product and elemental analysis by Energy Dispersive Spectroscopy and Fourier transform infrared spectroscopy. High crystallinity bacterial cellulose (81%) composed by high Iα confirmed by X-ray diffraction and solid state C13 nuclear magnetic resonance spectroscopy. The *Z*-average particle size was 1.44 μm with high porosity of 181.81%. The water holding and absorption capacity was determined. Tensile strength reveals a Young's modulus of 15.71 ± 0.15 MPa and tensile strength of up to 14.94 MPa. The thermal behavior evaluated by thermogravimetry and differential scanning calorimetry shows the thermal stability of bacterial cellulose. The results demonstrated unique characteristics of bacterial cellulose produced at shaking condition.

1. Introduction

Cellulose is the most abundant biopolymer on earth produced in large quantity in nature which is most commonly harvested from trees and cotton (Engelhardt, 1995). Bacteria belong to genera Agrobacterium, Rhizobium, Pseudomonas, Sarcina and Acetobacter can also synthesize cellulose (Cannon & Anderson, 1991). Unlike cellulose from plants, bacterial cellulose (BC) is chemically pure and free of lignin and hemi-cellulose. Plant-derived cellulose and BC have the same chemical composition but different structures and physical properties (Cannon & Anderson, 1991). As opposed to cotton and paper, where the purification of the cellulose product decreased the chain length, bacterial cellulose does not require remedial processing to remove unwanted polymers and contaminants (e.g. lignin, hemicellulose) and therefore, retains a greater degree of polymerization (Nishi et al., 1990). This fact gives bacterial cellulose superior unidirectional strength. *Acetobacter xylinum* produces two forms of cellulose: (i) cellulose I, the ribbon-like polymer, and (ii) cellulose II, which is thermodynamically more stable amorphous form of polymer (Brown, 1989). Cellulose I composed of parallel β, 1-4 glucan chains which are arranged uniaxially with van der Waals forces whereas β, 1-4 glucan chains of cellulose II are arranged in random manner. They are mostly antiparallel and with large number of hydrogen bonds that results in more stable form (Yu & Atalla, 1996). In nature, Cellulose I structure is found in allomorphic forms I_α or I_β, depending on the arrangement of the chains between each other. Cellulose belonging to plant cell walls shows higher percentage of I_β structure, compared with cellulose from algae and bacteria, that shows higher percentage of I_α structure, which seems to be a less stable displacement (Scionti, 2010). Normally *A. xylinum* cellulose displays characteristic of highly crystalline, I_α rich cellulose (VanderHart & Atalla, 1984). Microfibrillar structure of BC is responsible for most of its properties such as high tensile strength, high crystallinity index and higher degree of polymerization.

Due to specific properties such as the three dimensional nanomeric structure, unique physical, mechanical and thermal properties together with its higher purity BC has been commercialized as high end products like health food, high strength papers, audio speakers, filtration membranes, wound dressing materials, artificial skin, artificial blood vessels, and other biomedical devices (Czaja, Young, & Kawecki, 2007; Eming, Smola, & Kreig, 2002; Fontana et al., 1990; Okiyama, Motoki, & Yamanaka, 1993).

After 1990s research has been started for bacterial cellulose production focusing on its production, structural features, properties and applications. Suitable cultivation conditions (Bae & Shoda, 2004) and culture parameters (Jung, Park, & Chang, 2005; Son, Chung, Lee, & Kim, 2002) improve cellulose production. Bacterial cellulose has been produced under static or submerged shaking conditions (Chawla, Bajaj, Survase, & Singhal, 2009). In static

* Corresponding author. Tel.: +91 0257 2257421–25; fax: +91 257 2258403.
E-mail address: satish.patil7@gmail.com (S.V. Patil).

http://dx.doi.org/10.1016/j.carbpol.2014.02.012
0144-8617/

culture systems, BC production is low (Park, Jung, & Park, 2003) and requires more area, work force, and time, results into expensive production (Sani & Dahman, 2009). Shaking culture gives better BC production by improvement of cultural conditions (Son et al., 2003). Besides there are some problems with shaking culture like conversion into cellulose non producing mutants, many researchers suggested agitated culture as most economical for mass production (Ross, Mayer, & Benzimann, 1991; Yoshinaga, Tonouchi, & Watanabe, 1997). In our previous study we have optimized the production media and culture conditions for high BC production under shaking conditions (Mohite, Kamalja, & Patil, 2012; Mohite, Salunke, & Patil, 2013). The understanding of properties of BC will provide more opportunities in its widespread utilization. Hence it is necessary to study the characteristic properties of BC under shaking conditions. The characterization of BC produced under shaking condition has been previously tried with only few workers focusing on physical (Suwannapinunt, Burakorn, & Thaenthanee, 2007), Structural (Czaja, Romanovicz, & Brown, 2004), thermal and mechanical (Cheng, Catchmark, & Demirci, 2009) properties. It has been revealed that the characteristics of BC could be affected by many factors, such as media, fermentation modes and carbon sources. In our investigation we have studied the synthesis and structural characteristics of bacterial cellulose produced at shaking condition by *Gluconoacetobacter hansenii*. Morphological differences between the cellulose produced by static and agitated cultures contribute to varying degrees of crystallinity, different crystalline size and Iα cellulose content (Chawla et al., 2009). We try to explore the characteristics of bacterial cellulose produced at shaking condition such as the purity, structural, physical, mechanical and thermal properties along with determination of water absorbance and holding capacity, particle size, porosity and purity analysis. To the best of our knowledge this is one of the rare reports summarizing majority of the characteristics of BC produced under agitating conditions.

2. Materials and methods

2.1. Microorganism, production and purification of BC

G. hansenii (NCIM 2529) from National collection of industrial microorganisms, National Chemical Laboratory, Pune, India was used in this study. The *G. hansenii* from Hestrin Schramm (HS) agar slants inoculated into HS broth (pH 6.0). The flasks were incubated at 30 °C for 2 days at 120 rpm in an orbital shaking incubator. This is used as 5% (v/v) inoculum. In Previous study the production medium was statistically optimized (Mohite et al., 2012) and used here for production having composition as follows (in gram per liter): sucrose, 28.1; KNO_3, 5; Na_2HPO_4, 0.1 g; $CaCl_2$, 12.6; $MgSO_4$, 1 g with reaction parameters as: pH 3.88 temperature, 25 °C; incubation time, 5 days; agitation speed, 170 rpm. After incubation of 5 days, the produced beads of BC were separated by filtration and rinsed with distilled water to remove excess media, and then immediately boiled (at 90 °C) in 0.1 M NaOH solution for 30 min to remove the cells and medium embedded in the cellulose material. After boiling, the beads of BC were purified by extensive washing in distilled water at room temperature until the pH of the water became neutral. This obtained purified cellulose was lyophilized in powder form.

2.2. Characterization

2.2.1. Purity of bacterial cellulose

2.2.1.1. Thin layer chromatography (TLC) of hydrolysis product of bacterial cellulose. BC was treated with 8 N H_2SO_4 for 2 h. After hydrolysis of the polymer, the glucose monomers were detected by TLC with solvent system of ethyl acetate:propanol (65:35) with standard glucose as control and iodine was used as detecting agent (Zogaj et al., 2003).

2.2.1.2. Acetan (water soluble polysaccharide) detection. The harvested broth was centrifuged and bacterial cellulose beads were separated. The supernatant was mixed with ethanol in 1:3 proportions. The formation of precipitate of acetan was checked (Ishida, Sugano, Nakai, & Shoda, 2002).

2.2.2. Field emission scanning electron microscopy (FE-SEM) and Energy Dispersive Spectroscopy (EDS)

Scanning electron microscopy was used to determine the morphology and surface topography of the BC fibers, micrographs of the gold-coated samples of freeze dried BC were taken with a Field-emission scanning electron microscope (Hitachi S-4800, Japan). The element analysis was done by *Energy Dispersive Spectroscopy* (Brucker, Germany).

2.2.3. Fourier transform infrared spectroscopy (FTIR)

The BC produced by *G. hansenii* NCIM 2529 from our studies was mixed well with potassium bromide (KBr) powder and pressed into a small tablet. Fourier transform infrared spectroscopy (FT-IR) spectrum was recorded using a Shimadzu spectrometer (8400, Japan) in the transmittance mode with a resolution of 4 cm^{-1} in the range of 4000–400 cm^{-1}.

2.2.4. X-ray diffraction (XRD)

The freeze-dried samples were ground into powder for x-ray diffractometry analysis. The diffractograms were recorded at room temperature (Model D8 Advance, Brucker, corporation, Germany) using Ni-filtered Kα Cu X-ray radiation (λ = 1.54 Å). The operating voltage and current were 40 kV and 40 mA, respectively. Data were collected in reflection mode in the 10–40 2θ-range with a step of 0.02° 2θ intervals. The scans proceeded at 56.58 s per step. DIFRAC.EVA Suite software (Germany) was used to process the diffraction pattern and to calculate the crystallinity of BC.

2.2.5. Solid state C13 nuclear magnetic resonance (NMR) analysis

CP/MAS C13 NMR analysis was conducted on lyophilized sample using a spectrometer BRUKER DSX-300 solid state NMR spectrometer at −70 °C. The details of the instrument analysis are as follows: Magnetic field: 7.04 T, Platform: Linux & X-Winnmr, Proton freq.: 300.013 MHz, Carbon freq.: 75.47 MHz. Samples were packed in 7 mm ZrO_2 rotors and spun at 5 kHz. The experiments used recycle delays of 5 s, and each spectrum is the sum of 128 scans.

2.2.6. Mechanical analysis

The mechanical properties of the BC pellicles were analyzed through uniaxial tensile tests, using a testing machine Shimadzu AG-100KN, equipped with a biobath system containing distilled water, and a temperature-controlling system. The specimens were cut in a rectangular shape using a paper cutting machine, producing samples with dimensions of 1 cm × 5 cm individual sample thickness. A Bliss classic+ digital thickness indicator was used to measure the thickness of each specimen. Two samples were cut per pellicle, and three pellicles were used in each experimental session and average value was calculated f the three samples.

Using the Winsoft Tensile for Compression testing, connected to the Shimadzu machine, it was sufficient to insert the dimensions of the samples before the beginning of the experiments, and the software calculated automatically the values of stress and strain during the test. The Young's modulus was calculated using the same software, selecting manually the section of the stress–strain curves where it was required to measure it: the modulus was not measured

at the same value of strain, but it was calculated in the first linear part of the curve.

2.2.7. Water absorption capacity (WAC)

Water absorption capacity was determined by immersing the dried membranes in deionized water at room temperature until equilibration. After that the membranes were removed from the water & excess water at the surface of the membranes was blotted with blotting paper. The weight of the swollen membranes was measured and the procedure was repeated until no further weight change was observed (Saibuatong & Phisalaphong, 2010). The water content was calculated with the following formula,

$$\text{WAC}(\%) = \frac{W_h - W_d}{W_d} \times 100$$

when W_h and W_d denote the weight of hydrate and dry membrane respectively.

2.2.8. Water holding capacity (WHC)

Water holding capacity was determined as per shake method (Schrecker & Gostomski, 2005). The samples were shaken twice quickly and then weighed. The samples were dried at Room temperature for 48 h and their weights were measured at different time intervals. Then BC samples were dried for 12 h at 60 °C in order to completely remove water from them. Finally they were transferred quickly to the balance for weighing. WAC calculated by following formula, WHC = mass of water removed during drying (g)/dry weight of cellulose (g).

2.2.9. Thermogravimetric (TGA/DTG, DSC analysis)

Thermogravimetric analysis (TG and DTG) was carried out with a TGA 50, Shimadzu, Japan system. All analyses were performed with a 10 mg sample in 150 mm aluminum pans under a dynamic nitrogen atmosphere between 30 and 1000 °C. The experiments were run at a heating rate of 10 °C/min. The dynamic differential calorimetry (DSC) was analyzed with DSC 60, Shimadzu, Japan system. The nitrogen flow rate was 50 ml/min. The temperature range was −50 to 600 °C.

2.2.10. Particle size determination

The particle size of bacterial cellulose powder was determined with Zetasizer 2000 (Malvern, UK). The data was analyzed by Zetasizer Ver 6.34 software. Bacterial cellulose powder has poor flowability because of its tendency to absorb moisture and exhibits particles agglomeration. For this reason, the powder was prepared as dispersion by using a wet method. Readings were recorded in triplicate.

2.2.11. Porosity (%)

Dried BC were soaked in deionized water for more than 12 h at room temperature and the weight in water was measured by harnessing the sample in a device, which suspended the sample in water (Mancini, Bernsat, Sun, & Kucuk, 2001). The porosity was calculated by formula, Porosity (%) = (wet weight − dry weight)/(wet weight − wt in water) × 100.

3. Results and discussion

G. hansenii NCIM 2529 (ATCC 23769 – previously named *Acetobacter xylinus* and reclassified as *G. hansenii*) (Lisdiyanti, Navarro, Uchimura, & Komagata, 2006) is a Gram negative, strictly aerobic bacterium. It has been characterized and reported for cellulose production (Benziman, Haigler, White, & Cooper, 1980; Gromet-Elhanan & Hestrin, 1963). However, characterization of BC produced by this bacterium with different physicochemical properties has not been yet investigated.

The *G. hansenii* strain under agitated culture conditions produces cellulose in the form of characteristic spheres, as shown in Fig. 1a. The mechanism of cellulose production under agitating condition has not been fully resolved. The cells in fresh liquid medium attach around the air bubble and reproduce forming a cellulose ribbon results in a compact structure in the form of sphere. The shear force occurs during agitation causes the cells to separate from the surface of the spheres. The spherical BC produced at shaking condition has loose, porous hydrophilic network structure which provides more surface area to use as material for its repetitive utilization in interesting applications.

3.1. Confirmation of purity BC

3.1.1. Confirmation of purity by TLC of hydrolyzed product of BC

Purity of bacterial cellulose was confirmed by TLC after acid hydrolysis. The hydrolyzed product of bacterial cellulose (monomer sugar-glucose) was detected in comparison with standard glucose (Fig. 1b). The Rf value of hydrolyzed spot (1.90) matches with standard glucose (1.81). Hence it confirmed the bacterial cellulose, homopolymer of glucose produced by *G. hansenii*.

3.1.2. Detection of acetan production

The formation of acetan as a byproduct along with cellulose production was checked. There was no formation of solid mass in the form of precipitate was observed. Hence we concluded that the soluble polymer, acetan was not produced along with bacterial cellulose. *G. hansenii* was the solely produced polymer.

3.2. FE-SEM analysis

The field emission scanning electron micrograph showed a reticulated structure consisting of ultra fine cellulose fibrils. The strands are entangled and curved results in reticulated denser structure (Fig. 2a) while the fibers are highly extended at static production (Watanabe, Tabuchi, Morinaga, & Yoshinaga, 1998). These fibrils assembled together forming a porous structure with high aspect ratio. Nascent chains of BC aggregate to form subfibrils which are then crystallized into microfibrils, these into bundles, and the latter into ribbons (Park, Khan, & Jung, 2009). The morphological changes in BC beads affect the microstructures and various properties like the degree of polymerization, crystallinity, content of cellulose I and water holding capacity (Park et al., 2009; Watanabe et al., 1998).

3.3. EDS analysis

The obtained EDS spectrum in Fig. 2b shows the main element of the BC and these elements were identified as carbon and oxygen in 54.06 and 45.94 wt% respectively.

3.4. FT IR spectroscopy

FT-IR spectra of produced bacterial cellulose by G. hansenii NCIM 2529 was shown in Fig. 2c. The polymorphic form of bacterial cellulose reveals by the position and intensity of peaks in the FTIR spectra. Characteristic absorption peaks of bacterial cellulose are at 3350 cm^{-1} showed several bands typical for cellulose in the region of 1500–1235 cm^{-1} due to O—H stretching and at 2960 cm^{-1} due to CH stretching. The band at 1653.8 cm^{-1} is due to deformation vibration of the absorbed water molecules. The band at 1068 cm^{-1} could be associated with ether C—O—C functionalities as investigated earlier by Wonga, Kasapis, and Tan (2009).

According to Nelson and O'Connor (1964), a weak and broad band centered at 891.59 cm^{-1} and a strong band centered at 1424.18 cm^{-1} (CH_2 scissoring) in the spectra of the microbial cellulose samples, defining them as cellulose I. BC at both shaking and

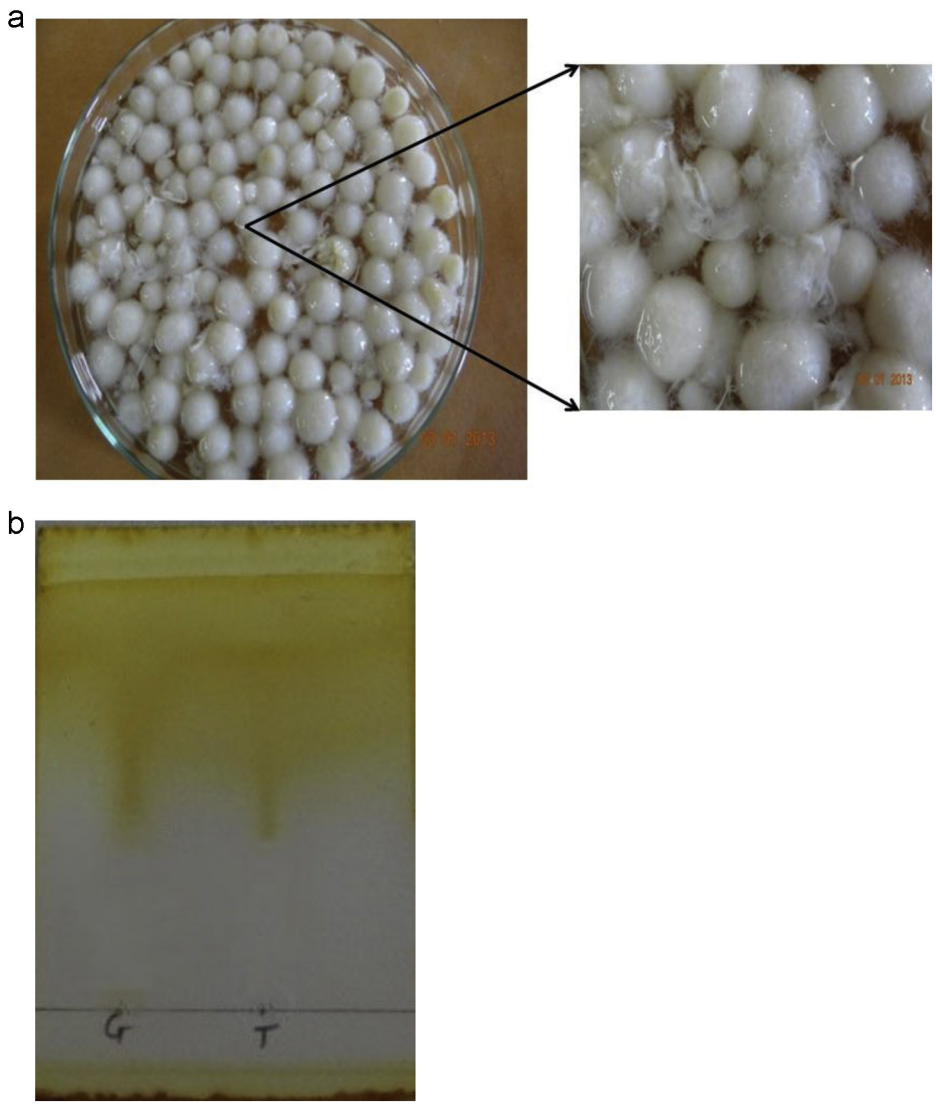

Fig. 1. (a) BC spheres produced under the agitated culture condition. (b) TLC of hydrolyzed product (glucose) of BC.

static condition has a form of cellulose I representing pure cellulose (Moon, Park, Chun, & Kim, 2006). All the above characteristics of FT-IR spectrum and comparison with the available literature suggest that the produced component by *G. hansenii* in the present study is bacterial cellulose.

3.5. XRD analysis

Generally, native cellulose is composed by two allomorphs, a mixture of Iα and Iβ phases, which ratio depends on the species and source. For instance, Iα structure is prevalent in cellulose produced by algae and bacteria whereas Iβ is dominant in cellulose obtained from woods (Nishiyama, Sugiyama, Chanzy, & Langan, 2003; Zugenmaier, 2001). Broad diffraction peaks at 15 and 22.5° are assigned to the characteristic interplane distances of cellulose Iα and Iβ phases (100Iα, 110Iβ and 010Iβ planes at 15° and 110Iα and 200Iβ at 22.5°) (Fig. 3a). The XRD of commercial wood cellulose presents a diffraction peak located at 34.5° which is ascribed to Iβ phase (Andersson, Ritva Serimaa, Paakkari, Saranpää, & Pesonen, 2003). The low intensity of this peak suggest that it mainly comprised of Iα native cellulose. These results are in agreement with Horii, Hirai, and Yamamoto (1997), who reported native cellulose produced by *A. xylinum* composed by 64% of Iα and 36% of Iβ phases. XRD patterns obtained from our BC samples demonstrated three main characteristic peaks standing for crystal plane $\langle 1\bar{1}0 \rangle$, ⟨010⟩, and ⟨020⟩ (Fig. 6), which showed that the cellulose exhibited primarily the Iα pattern (Czaja et al., 2004).

The crystallinity index was found to be 81.2% and the crystal size of ⟨200⟩ crystal plane remained the same around 5.2 nm by the use of DIFRAC.EVA Suite software. The diffraction patterns were indexed according to the cellulose I indexation described by Sugiyama, Persson, and Chanzy (1991). The three visible peaks were assigned to $\langle 1\bar{1}0 \rangle$, ⟨010⟩, and ⟨020⟩ crystallographic planes, corresponding to diffraction angles of 14.56°, 16.87 and 22.74, respectively as proposed by Isogai (1994). The calculated interplanar crystal distances (d-spacings) and crystallite dimensions are listed in Table 1.

3.6. Solid state C13 NMR analysis

CP/MAS is the technique useful for structural investigation of bacterial cellulose. The NMR spectrum was shown in Fig. 3b.

The singlet peak of C-1 in the spectrum of BC at agitated culture appeared at 106.0 ppm and that of C-6 at 54.02 ppm prove the cellulose I lattice (Keshk, 2008). This indicates that cellulose

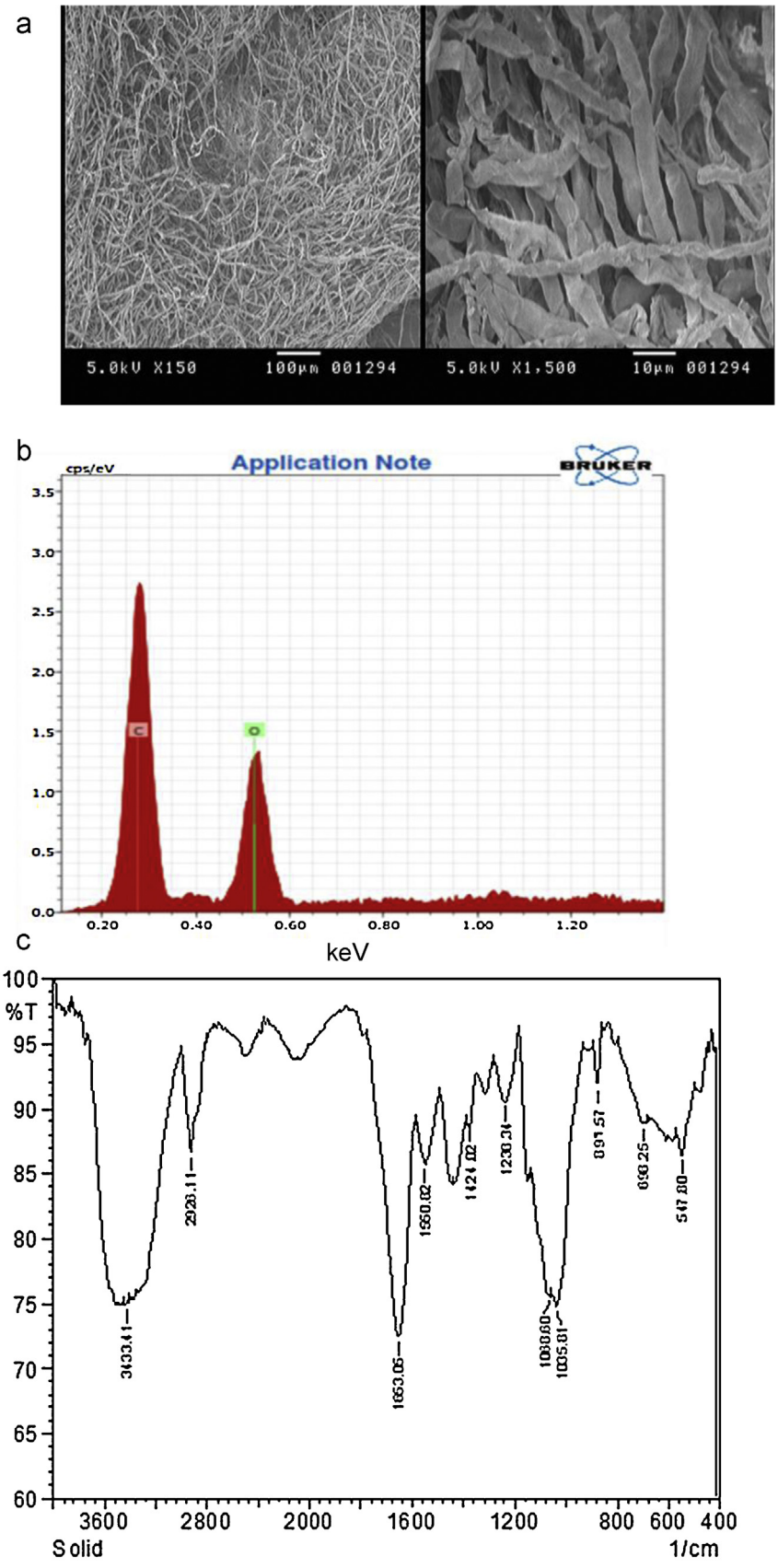

Fig. 2. (a) FE-SEM micrographs of the morphology of BC. (b) EDS spectrum showing purity of BC. (c) FT-IR spectrum of BC.

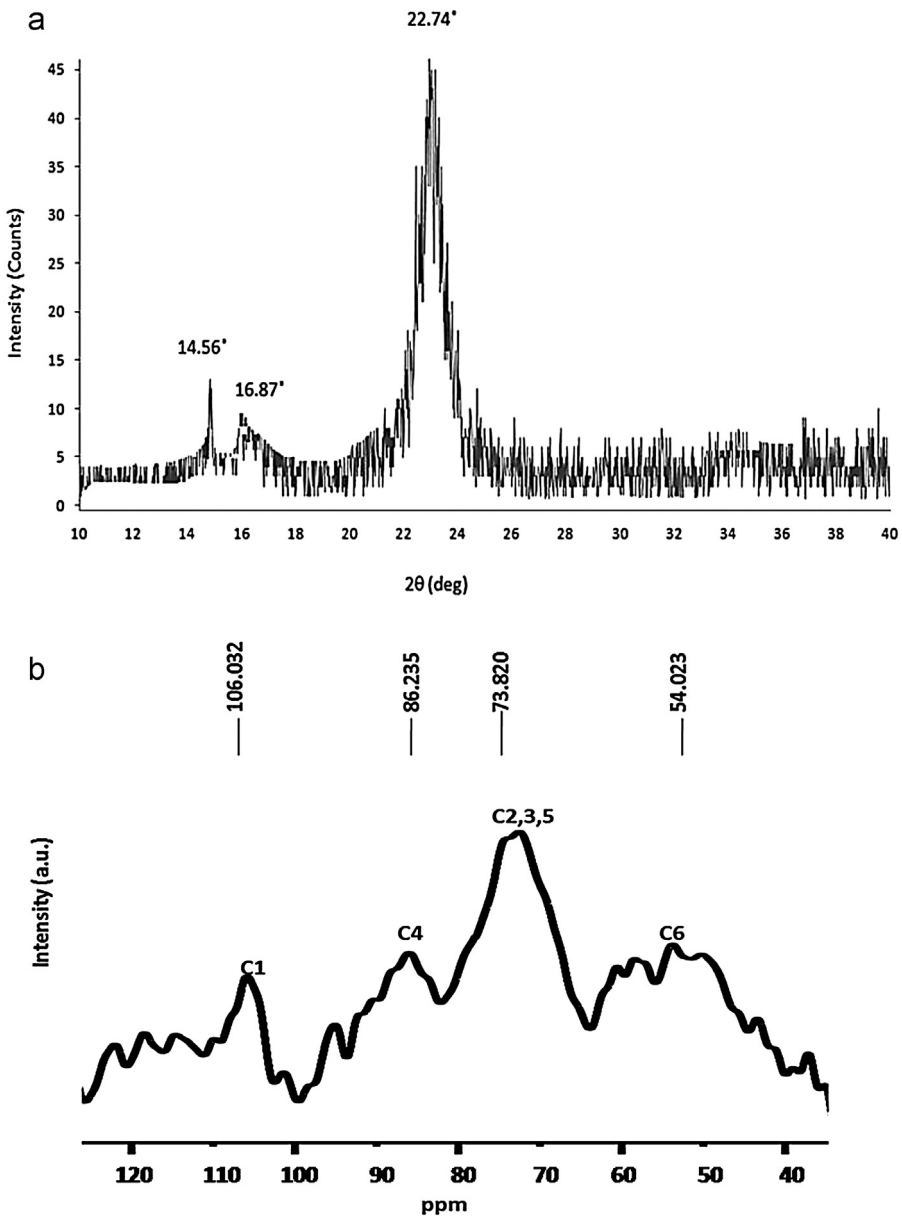

Fig. 3. (a) X-ray diffraction pattern of BC. (b) CP/MAS C13 NMR spectra of BC.

Iα is dominant in the sample. Furthermore, the peaks at 86.2 ppm are due to amorphous regions of C-4. Amorphous cellulose parts were found near 86.23 ppm (C4 region), and between 58.6 and 54.02 ppm (C6 region) for the BC from *G. hansenii*. The chemical shifts of 73.82 ppm and 74.5 ppm are attributed to C-2, 3, 5 (Hesse-Ertelt, Witter, Ulrich, Kondo, & Heinze, 2008). The high crystallinity of bacterial cellulose affects the sharpness of the signals. Bacterial cellulose represents high crystalline celluloses, with high Iα content, also as published earlier (Lennholm, Larsson, & Iversen, 1994; Lennholm, Wallbäcks, & Iversen, 1995).The low amount of cellulose II which was detected in the spectrum of bacterial cellulose is difficult to explain, but recently its occurrence has been suggested in the literature (Shibazaki, Saito, Kuga, & Okano, 1998). The content of cellulose Iα was reported lower in shaking condition compared with static condition (Czaja et al., 2004). The interference in the crystallization process of BC may lead to the formation of crystallites of a smaller size; as a result of this the formation process of cellulose I_β may be preferentially induced. Although shaking condition results into lower content of cellulose Iα, smaller size of crystallites that leads to smaller particles, but it has higher retention aid function in paper making process, it could be used as a carrier to adsorb or cross link substances like cells, enzymes and proteins, due to wider accessible surface area of BC sphere (Watanabe et al., 1998; Zhu et al., 2011).

Table 1
Crystallinity index, *d* spacing of BC produced under agitating condition determined from X-ray diffractograms.

Sample	CI	2θ [*d*1 (1$\bar{1}$0)]	2θ [*d*2 (010)]	2θ [*d*3 (020)]
BC	81.2	14.56(6.08 Å)	16.87° (5.25 Å)	22.74°(3.91 Å)

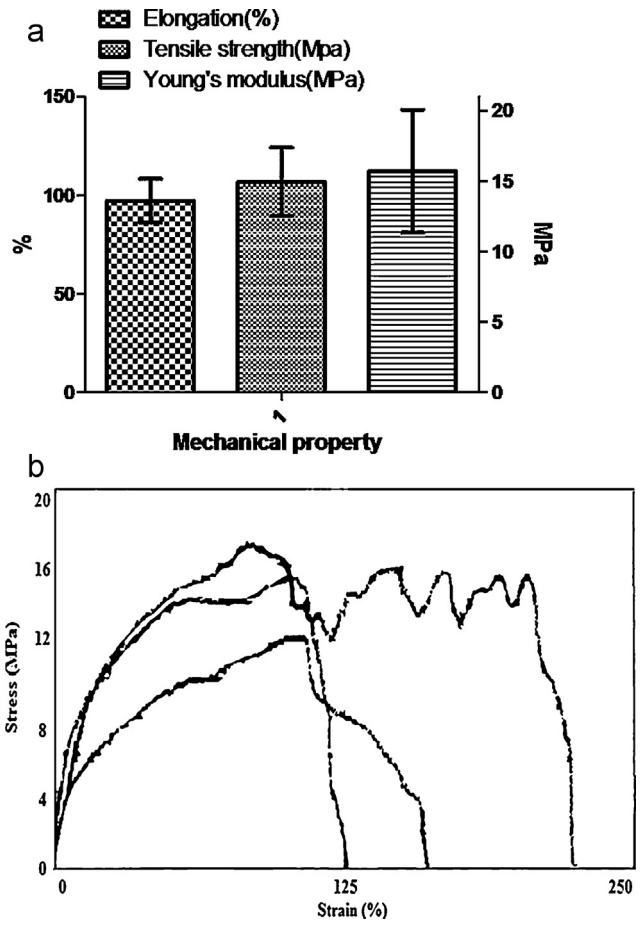

Fig. 4. (a) Stress strain curve of BC (sample in triplicate). (b) Tensile strength, Young's modulus and elongation of BC.

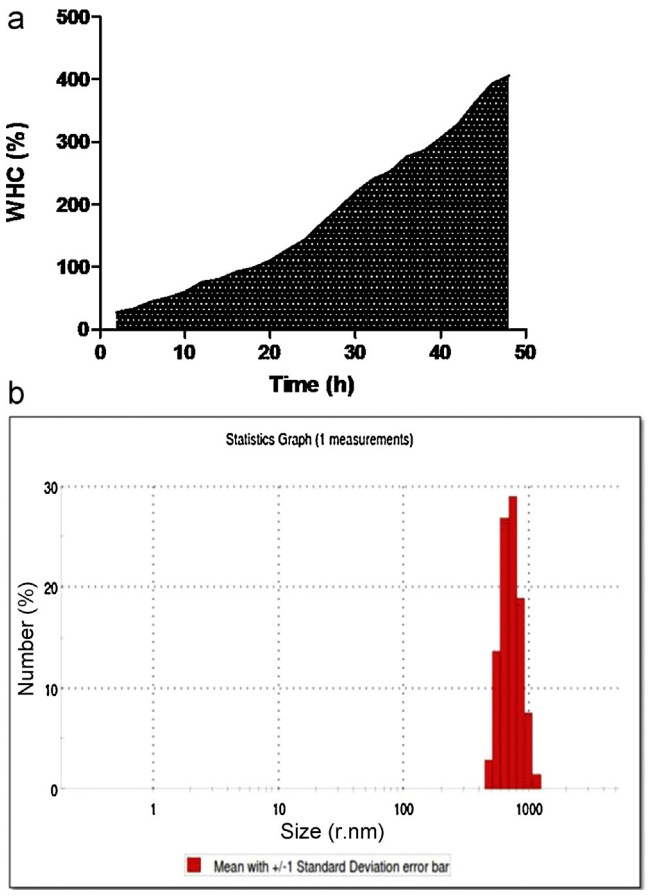

Fig. 5. (a) WHC profile of BC with relative time period. (b) *Z*-average particle size distribution of BC.

3.7. Mechanical strength

Tensile tests provide important information regarding the mechanical properties of a material, and are commonly used in for analyses of new materials for engineering applications, as they are very effective methods to compare the properties of different materials. The maximum load was 11.95 ± 0.2 N and maximum displacement was 9.71383 ± 0.11 mm respectively (Table 2).

The maximum stress applied was 14.94 ± 0.08 N/mm^2 that results into maximum strain of 97.13 ± 0.18%. Theoretically Young's modulus is 173 GPa and tensile strength in the order of 2 GPa (Yamanaka et al., 1989). These mechanical properties are based on a pure cellulose fiber and therefore, they are never reached in actual materials that consist of cellulose fibers. The elongation % was very high (97.13 ± 0.2) and the Young's modulus calculated from slope of stress and strain curve was 15.71 N/mm^2 (Fig. 4a and b). Watanabe et al. (1994) proposed that there is a strong relation correlation between crystallinity of BC and Young's modulus of its sheet.

The grater tensile strength is due to large amount of polymerization. The material elongation can be attributed to the fact that the water existing in the material matrix allows the cellulose fibers to slide over each other. BC is a random in-the-plane orientation of nanofibrils (Son et al., 2002). It was also considered as 3D interwoven network of nanofibrils, "extremely fine, pure and dimensionally uniform" (Nakagaito, Iwamoto, & Yano, 2005). These results proved bacterial cellulose as a material with the beneficial properties of strength and stiffness.

3.8. Water absorption capacity (WAC), water holding capacity (WHC)

The ability to absorb high amount of water is important but to retain the water for long period of time is also important. This property helps the biopolymer to work as biomaterial as antimicrobial wound dressing to absorb high amount of antibiotic solution and slowly release it at wound site by holding it for longer period of time. The presence of moisture enables easy and painless dressing change without damage to newly formed skin (Newman, 1998).

The water absorption capacity for bacterial cellulose was calculated as 400%. Bacterial cellulose is a hydrophilic material as it can generate capillary force to suck the water molecules due to its physical structure which generate the capillary force to suck the molecules of water (Klemm, Schumann, Udhardt, & Marsch, 2001).

The thinner fiber nature of BC was demonstrated by SEM morphology. The thinner and longer fibers having large surface area hold more water. The water holding capacity was measured as 400 times its dry weight (400 ± 0.4%) which increases proportionally with increase in time (Fig. 5a). Due to extensive hydrogen bonding within the reticulated network, it can hold water upto 400 times of its dry weight in water. The water is trapped physically at the surface and on the inside of the particles composed of the reticulated fibrils. Under any of the conditions applied water holding capacity of BC at shaking was reported higher than at static (Watanabe et al., 1998).

Table 2
Mechanical properties of BC determined by Universal testing machine.

Sample	Thickness (μm)	Max load (N)	Max displacement (mm)	Max stress (MPa)	Max strain (%)	% Elongation	Young's modulus (MPa)
BC	350 ± 0.43	11.95 ± 0.2	9.71 ± 0.11	14.94 ± 0.08	97.13 ± 0.18	97.13 ± 0.23	15.71 ± 0.15

Sample size (n) = 3.

3.9. Particle size

The Z-average particle size was 1.44 μm having maximum particles of size 0.7419 μm. The particle size distributed between 0.4777 μm and 1.152 μm (Fig. 5b). The small particle size of BC in comparison with BC produced at static condition increases the surface area enhance the remarkable properties of it like high water absorption capacity, water holding capacity, porosity etc.

The cellulose fibers extruded through the 100 μm sieve to form irregular fibrous, fluffy powder. Standard powder cellulose from Sigma, microcrystalline cellulose or cotton linters have granular structure and thus the particle size can be directly determined using SEM. However, the fibrous structure of bacterial cellulose powder has irregular morphology and thus the particle size need to be determined via a different approach (Halib, Amin, & Ahmad, 2012). Moreover because the powder shows poor flowability, the test was performed using wet method in which the cellulose was dispersed in distilled water. Bacterial cellulose has a tendency to swell due to many hydroxyl group which interact with water by formation of hydrogen bonds; thus, the bacterial cellulose has a tendency to swell. Hence, for accurately determining the particle size, the value acquired by this method should consider the swelling power of the cellulose fibers (Stana-Kleinschek, Kreze, Ribitsch, & Strnad, 2001).

3.10. Porosity

The porosity of BC was calculated as 181.81%. The three dimensional non oven structure with large amount of pores which is maintained by freeze drying is responsible for highly porous nature which allows its application as wound dressing material and release of drug (Iguchi, Yamanaka, & Budhiono, 2000).

3.11. Thermal analysis (TGA/DTG, DSC analysis)

3.11.1. TGA

Thermo-gravimetric analysis (TGA) is a continuous process, involving the measurement of sample weight in accordance with increasing temperature in the form of programmed heating. The TGA curves obtained by plotting percentage weight loss against temperature indicated one step decomposition process showing BC was stable up to a temperature of 220 °C (Fig. 6a).

The bacterial cellulose showed maximum rate of weight loss at 303.2 °C (95%). With increasing temperature the weight of bacterial cellulose decreased slowly at first. As the temperature increase from ambient to 200 °C, fibers desorbed the physically absorbed water. Such water was mainly associated with the amorphous areas, and the crystalline areas generally do not absorb water. The percentage weight loss for BC at 120 °C was 8%, while 66% weight loss was noticed at 282 °C and maximum rate of weight loss at 303.2 °C (95%). The thermal degradation temperature is affected by the structural parameters such as molecular weight, crystallinity and orientation.

The internal structure was compact so the physically absorbed water gradually decreased. The first reaction is dehydration of cellulose, an endothermic process known as dehydrocellulose (Kilzer & Broido, 1965). After that, depolymerization results into levoglucosan (1,6-anhydro-β-D-glucopyranose) as an essential intermediate. Dehydrocellulose that was produced in the previous reaction was then results into gaseous products (CO, CO_2) and residual char (Arseneau, 1971).

Additionally, a derivative of TG curve (DTG) was shown as well. The DTG curve shows that the maximum rate of this transformation occurs at temperature of approximately 300 °C.

3.11.2. Differential scanning colorimetry (DSC)

DSC measures the heat absorbed or released by a material as a function of temperature or time (isothermally). Glass transition temperature (Tg) of BC films was found to be 44.28 °C (Fig. 6b) which is higher than reported by George, Ramana, Sabapathy, Jagannath, and Bawa (2005) for native (13.94 °C) and NaOH treated (41.41 °C) BC membrane but it was lower than the benzoylated bacterial cellulose (280 °C) as reported by Wang, Luo, Peng, and Pei (2008).

Higher Tg is advantageous because minimal aging is expected at storage temperature (which is well below the Tg) (Béchard, Levy, & Clas, 1995). According to literature, at a temperature of 80–140 °C, there is a known transformation related to the melting of the crystalline phase of cellulose (George et al., 2005). Tm occurs at 84.44 °C.

No degradation peaks were detected upto the temperature range 300 °C. Crystallization peak occurs at 343.06 °C (*Tc*). On further heating, polymorphic transition can occur before the solid phase finally melts. Next exothermic transformation proceeds with decomposition peak at 487.85 °C. The high thermal stability might

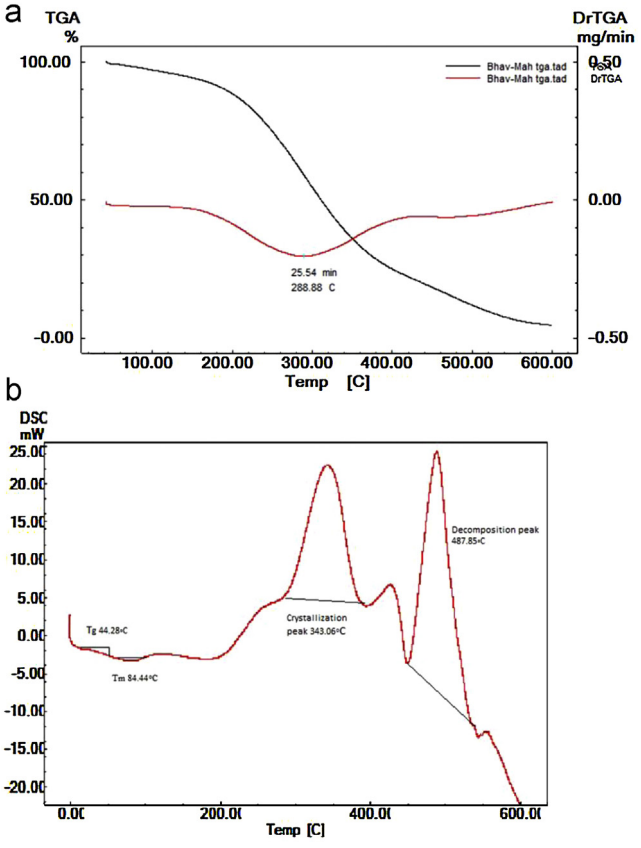

Fig. 6. (a) TG and DTG spectrum of BC. (b) DSC spectrum of BC.

be attributed to the high crystallinity, highly orientated cellulose chains within fibrils, and pure cellulosic form (Chen, Kim, Kwon, Yun, & Jin, 2009; Hsieh, Cyano, Nogi, & Eichhorn, 2008).

4. Conclusion

Bacterial cellulose was prepared from *G. hansenii* by shaking culture conditions in order to analyze its physico mechanical, structural and thermal characteristics. The combination of several analysis results allowed analyzing the behavior of BC for high performance applications. It is thought that the results of this study help to comprehend the characteristic potential of bacterial cellulose produced at less exploited shaking condition. The FTIR, NMR and XRD spectra revealed purity of bacterial cellulose showing cellulose Iα type with high crystalline nature. SEM EDS, particle size and porosity determination confirmed the highly reticulated porous structure with miniature particles. The nanostructured material show higher mechanical properties established by tensile strength and Young's modulus measurement. Thermal stable nature with high moisture retention ability was verified by thermogravimetric analysis and by WHC and WAC measurement. BC produced at shaking condition exhibits more suitable properties with regard to higher water holding capacity, smaller particle size in support to its wide range of applications. The acquaintance of its novel properties will provide more opportunities in its widespread utilization.

Acknowledgment

The research fellowship to Bhavna Mohite from University Grants Commission, New Delhi under the Research Fellowship in Sciences for meritorious students' scheme is gratefully acknowledged.

References

Andersson, S., Ritva Serimaa, R., Paakkari, T., Saranpää, P., & Pesonen, E. (2003). Crystallinity of wood and the size of cellulose crystallites in Norway spruce (*Picea abies*). *Journal of Wood Science*, *49*, 531–537.

Arseneau, F. D. (1971). Competitive reaction in the thermal decomposition of cellulose. *Canadian Journal of Chemistry*, *49*, 632–638.

Bae, S. O., & Shoda, M. (2004). Bacterial cellulose production by fed batch fermentation in molasses medium. *Biotechnology Progress*, *20*(5), 1366–1371.

Béchard, S. R., Levy, L., & Clas, S. D. (1995). Thermal, mechanical and functional-properties of cellulose-acetate phthalate (CAP) coatings obtained from neutralized aqueous-solutions. *International Journal of Pharmaceutics*, *114*(2), 205–213.

Benziman, M., Haigler, C. H. B., Jr., White, A. R., & Cooper, K. M. (1980). Cellulose biogenesis: Polymerization and crystallization are coupled processes in *Acetobacter xylinum*. *Proceedings of the National Academy of Sciences of the United States of America*, *77*(11), 6678–6682.

Brown, R. M., Jr. (1989). Bacterial cellulose. In Kennedy, Phillips, & Williams (Eds.), *Cellulose: Structural and functional aspects* (pp. 145–151). Chichester, UK: Ellis Horwood Ltd.

Cannon, R. E., & Anderson, S. M. (1991). Biogenesis of bacterial cellulose. *Critical Reviews in Microbiology*, *17*(6), 435–447.

Chawla, P. R., Bajaj, I. B., Survase, S. A., & Singhal, R. S. (2009). Microbial cellulose: Fermentative production and applications. *Food Technology and Biotechnology*, *47*(2), 107–124.

Chen, P., Kim, H.-S., Kwon, S.-M., Yun, Y. S., & Jin, H.-J. (2009). Regenerated bacterial cellulose/multi-walled carbon nanotubes composite fibers prepared by wet-spinning. *Current Applied Physics*, *9*(2 (Suppl. 1)), 96–99.

Cheng, K. C., Catchmark, J. M., & Demirci, A. (2009). Enhanced production of bacterial cellulose by using a biofilm reactor and its material property analysis. *Journal of Biological engineering*, *3*(12), 1–10.

Czaja, W. K., Young, D. J., & Kawecki, M., Jr. (2007). The future prospects of microbial cellulose in biomedical applications. *Biomacromolecule*, *8*, 1–12.

Czaja, W., Romanovicz, D., & Brown, R. M. (2004). Structural investigations of microbial cellulose produced in stationary and agitated culture. *Cellulose*, *11*, 403–411.

Eming, S., Smola, H., & Kreig, T. (2002). Treatment of chronic wounds: State of the art and future concepts. *Cells, Tissues, Organs*, *172*, 105–117.

Engelhardt, J. (1995). Sources, industrial derivatives and commercial application of cellulose. *Carbohydrates in Europe*, *12*, 5–14.

Fontana, J. D., de Sousa, A. M., Fontana, C. K., Torriani, I. L., Moreschi, J. C., Gallotti, B. J., et al. (1990). Acetobacter cellulose pellicle as a temporary skin substitute. *Applied Biochemistry and Biotechnology*, *25*, 253–264.

George, J., Ramana, K. V., Sabapathy, S. N., Jagannath, J. H., & Bawa, A. S. (2005). Characterization of chemically treated bacterial (*Acetobacter xylinum*) biopolymer: Some thermo-mechanical properties. *International Journal of Biological Macromolecules*, *37*(4), 189–194.

Gromet-Elhanan, Z., & Hestrin, S. (1963). Synthesis of cellulose by *Acetobacter xylinum*. VI. Growth on citric acid-cycle intermediates. *Journal of Bacteriology*, *85*, 284–292.

Halib, N., Amin, M. C. I. M., & Ahmad, I. (2012). Physicochemical properties and characterization of nata de coco from local food industries as a source of cellulose. *Sains Malaysiana*, *41*(2), 205–211.

Hesse-Ertelt, S., Witter, R., Ulrich, A. S., Kondo, T., & Heinze, T. (2008). Spectral assignments and anisotropy data of cellulose I (alpha): ^{13}C-NMR chemical shift data of cellulose I (alpha) determined by INADEQUATE and RAI techniques applied to uniformly ^{13}C-labeled bacterial celluloses of different *Gluconacetobacter xylinus* strains. *Magnetic Resonance in Chemistry*, *46*, 1030–1036.

Horii, F., Hirai, A., & Yamamoto, H. (1997). Microstructural analysis of microfibrils of bacterial cellulose. *Macromolecular Symposium*, *120*, 197–205.

Hsieh, Y., Cyano, H., Nogi, M., & Eichhorn, S. J. (2008). An estimation of the Young's modulus of bacterial cellulose filaments. *Cellulose*, *15*(4), 507–513.

Iguchi, M., Yamanaka, S., & Budhiono, A. (2000). Bacterial cellulose – A masterpiece of nature's arts. *Journal of Materials Science*, *35*, 261–270.

Ishida, T., Sugano, Y., Nakai, T., & Shoda, M. (2002). Effects of acetan on production of bacterial cellulose by *Acetobacter xylinum*. *Bioscience, Biotechnology, and Biochemistry*, *66*(8), 1677–1681.

Isogai, I. (1994). In R. D. Gilbert (Ed.), *Cellulosic polymers, blends and composite* (pp. 5–23). USA: Hanser/Gardner Publications.

Jung, J. Y., Park, J. K., & Chang, H. N. (2005). Bacterial cellulose production by *Gluconacetobacter hansenii* in an agitated culture without living non-cellulose producing cells. *Enzyme Microbiology Technology*, *37*(3), 347–354.

Keshk, S. M. A. S. (2008). Homogenous reaction of cellulose from different natural sources. *Carbohydrate Polymers*, *74*, 942–945.

Kilzer, F. J., & Broido, A. (1965). Speculations on the nature of cellulose pyrolysis. *Pyrodynamics*, *2*, 151–163.

Klemm, D., Schumann, D., Udhardt, U., & Marsch, S. (2001). Bacterial synthesized cellulose artificial blood vessels for microsurgery. *Progress in Polymer Science*, *26*, 1561–1603.

Lennholm, A., Larsson, T., & Iversen, T. (1994). Determination of cellulose Iα and Iβ in lignocellulosic materials. *Carbohydrate Research*, *261*, 19–131.

Lennholm, A., Wallbäcks, L., & Iversen, T. (1995). Solid-state high-resolution ^{13}C-NMR studies of regenerated cellulose samples with different crystallinities. *Nordic Pulp and Paper Research Journal*, *10*, 46–50.

Lisdiyanti, P., Navarro, R. R., Uchimura, T., & Komagata, K. (2006). Reclassification of *Gluconacetobacter hansenii* strains and proposals of *Gluconacetobacter saccharivorans* sp. nov. and *Gluconacetobacter nataicola* sp. nov. *International Journal of Systematic and Evolutionary Microbiology*, *56*, 2101–2111.

Mancini, C. E., Bernsat, C. C., Sun, L., & Kucuk, A. (2001). Porosity determinations in thermally sprayed hydroxyapatite coatings. *Journal of Materials Science*, *36*(16), 3891–3896.

Mohite, B. V., Salunke, B. K., & Patil, S. V. (2013). Enhanced production of bacterial cellulose by using *Gluconacetobacter hansenii* NCIM 2529 strain under shaking conditions. *Applied Biochemistry and Biotechnology*, *169*, 1497–1511.

Mohite, B. V., Kamalja, K. K., & Patil, S. V. (2012). Statistical optimization of culture conditions for enhanced bacterial cellulose production by *Gluconoacetobacter hansenii* NCIM 2529. *Cellulose*, *19*, 1655–1666.

Moon, S., Park, J., Chun, H., & Kim, S. (2006). Comparison of physical properties of bacterial celluloses produced in different culture conditions using saccharified food wastes. *Biotechnology and Bioprocess Engineering*, *11*, 26–31.

Nakagaito, A. N., Iwamoto, S., & Yano, H. (2005). Bacterial cellulose: The ultimate nano-scalar cellulose morphology for the production of high-strength composites. *Applied Physics A*, *80*, 93–97.

Nelson, M. L., & O'Connor, R. T. (1964). Relation of certain infrared bands to cellulose crystallinity and crystal latticed type. Part I. Spectra of lattice types I, II, III and of amorphous cellulose. *Journal of Applied Polymer Science*, *8*, 1311–1324.

Newman, R. H. (1998). Evidence for assignment of ^{13}C NMR signals to cellulose crystallite surfaces in wood, pulp and isolated celluloses. *Holzforschung*, *52*, 57–159.

Nishi, Y., Uryu, M., Yamanaka, S., Watanabe, K., Kitamura, N., Iguchi, M., et al. (1990). The structure and mechanical properties of sheets prepared from bacterial cellulose. 2. Improvement of the mechanical properties of sheets and their applicability to diaphragms of electroacoustic transducer. *Journal of Materials Science*, *25*(6), 2997–3001.

Nishiyama, Y., Sugiyama, J., Chanzy, H., & Langan, P. (2003). Crystal structure and hydrogen bonding system in cellulose I(alpha) from synchrotron X-ray and neutron fiber diffraction. *Journal of the American Chemical Society*, *125*(47), 14300–14306.

Okiyama, A., Motoki, M., & Yamanaka, S. (1993). Bacterial cellulose IV. Application to processed foods. *Food Hydrocolloids*, *6*, 503–511.

Park, J. K., Jung, J. Y., & Park, Y. H. (2003). Cellulose production by *Gluconacetobacter hansenii* in a medium containing ethanol. *Biotechnology Letters*, *25*(24), 2055–2059.

Park, J. K., Khan, T., & Jung, J. (2009). In G. O. Phillips, & P. A. Williams (Eds.), *Handbook of hydrocolloids* (3rd ed., pp. 724–739). Cambridge, UK: Woodhead Publishing Limited.

Ross, P., Mayer, R., & Benzimann, M. (1991). Cellulose biosynthesis and function in bacteria. *Microbiological Reviews*, *55*, 35–58.
Saibuatong, O., & Phisalaphong, M. (2010). Novo aloe vera-bacterial cellulose composite film from biosynthesis. *Carbohydrate Polymers*, *79*, 455–460.
Sani, A., & Dahman, Y. (2009). Improvements in the production of bacterial synthesized biocellulose nanofibres using different culture methods. *Journal of Chemical Technology and Biotechnology*, *85*, 151–164.
Schrecker, S. T., & Gostomski, P. A. (2005). Determining the water holding capacity of microbial cellulose. *Biotechnology Letters*, *27*, 1435–1438.
Scionti, G. (2010). *Mechanical properties of bacterial cellulose implants* (Master of Science thesis in biomedical engineering). Göteborg, Sweden: Chalmers University of Technology.
Shibazaki, H., Saito, M., Kuga, S., & Okano, T. (1998). Native cellulose II production by *Acetobacter xylinum* under physical constraints. *Cellulose*, *5*, 65–173.
Son, C., Chung, S., Lee, J., & Kim, S. (2002). Isolation and cultivation characteristics of *Acetobacter xylinum* KJ-1 producing bacterial cellulose in shaking culture. *Journal of Microbiology and Biotechnology*, *12*(5), 722–728.
Son, H. J., Kim, H. G., Kim, K. K., Kim, H. S., Kim, Y. G., & Lee, S. J. (2003). Increased production of bacterial cellulose by *Acetobacter* sp. V6 in synthetic media under shaking culture conditions. *Bioresource Technology*, *86*(3), 215–219.
Stana-Kleinschek, K., Kreze, T., Ribitsch, V., & Strnad, S. (2001). Surface characterization of NH_3 plasma treated polyamide 6 foils. *Colloids and Surfaces A*, *195*, 275–284.
Sugiyama, J., Persson, J., & Chanzy, H. (1991). Combined infrared and electron diffraction study of the polymorphism of native celluloses. *Macromolecules*, *24*(9), 2461–2466.
Suwannapinunt, N., Burakorn, J., & Thaenthanee, S. (2007). effect of culture conditions on bacterial Cellulose (BC) production from *Acetobacter xylinum* tistr976 and physical properties of BC parchment paper. *Suranaree Journal of Science and Technology*, *14*(4), 357–436.
VanderHart, D. L., & Atalla, R. H. (1984). Studies of microstructure in native cellulose using solid state ^{13}C NMR. *Macromolecules*, *17*, 1465–1472.
Wang, Y., Luo, Q., Peng, B., & Pei, C. (2008). A novel thermotropic liquid crystalline – Benzoylated bacterial cellulose. *Carbohydrate Polymers*, *74*(4), 875–879.
Watanabe, K., Hori, Y., Tabuchi, M., Morinaga, Y., Yoshinaga, F., Horii, F., et al. (1994). Structural features of bacterial cellulose vary depending on the culture conditions. In *Proceedings of '94 Cellulose R & D, 1st annual meeting of cellulose society of Japan* (pp. 45–50).
Watanabe, K., Tabuchi, M., Morinaga, Y., & Yoshinaga, F. (1998). Structural features and properties of bacterial cellulose produced in agitated culture. *Cellulose*, *5*, 187–200.
Wonga, S. S., Kasapis, S., & Tan, Y. M. (2009). Bacterial and plant cellulose modification using ultrasound sonication. *Carbohydrate Polymers*, *77*, 280–287.
Yamanaka, S., Watanabe, K., Kitamura, N., Iguchi, M., Mitsuhashi, S., Nishi, Y., et al. (1989). *Journal of Materials Science*, *24*, 3141–3145.
Yoshinaga, F., Tonouchi, N., & Watanabe, K. (1997). Research progress in production of bacterial cellulose by aeration and agitation culture and its application as a new industrial material. *Bioscience Biotechnology Biochemistry*, *61*, 219–224.
Yu, X., & Atalla, R. H. (1996). Production of cellulose II by *Acetobacter xylinum* in the presence of 2,6-dichlorobenzonitrile. *International Journal of Biological Macromolecules*, *19*, 145–146.
Zhu, H., Jia, S., Yang, H., Jia, Y., Yan, L., & Li, J. (2011). Preparation and application of bacterial cellulose sphere: A novel biomaterial. *Biotechnology and Biotechnological Equipment*, http://dx.doi.org/10.5504/bbeq.2011.0010OI
Zogaj, X., Bokranz, W., Nimtz, M., & Romling, U. (2003). Production of cellulose and curli fimbriae by members of the family *Enterobacteriaceae* isolated from the human gastrointestinal tract. *Infection and Immunity*, *71*(July (7)), 4151–4158.
Zugenmaier, P. (2001). Conformation and packing of various crystalline cellulose fibers. *Progress in Polymer Science*, *26*, 1341–1417.